1-1-1981

Tunable Optical Filter Using an Interferometer for Selective Modulation

Roy W. Esplin
Utah State University

Ronald J. Huppi
Utah State University

Marshall H. Bruce
Utah State University

George A. Vanasse

Esplin, Roy W., Ronald J. Huppi, and Marshall H. Bruce. 1981. "Tunable Optical Filter Using an Interferometer for Selective Modulation." *Proceedings of SPIE* 268: 129–39. doi:10.1117/12.959935.

Tunable optical filter using an interferometer for selective modulation

Roy W. Esplin, Ronald J. Huppi, Marshall H. Bruce
Stewart Radiance Laboratory, Utah State University
1 DeAngelo Drive, Bedford, Massachusetts 01730

George A. Vanasse
Air Force Geophysics Laboratory
Hanscom Air Force Base, Bedford, Massachusetts 01731

Abstract

Using the selective modulation interferometric spectrometer (SIMS) as a tunable filter is proposed. This tunable filter can have a large optical throughput and a resolving power on the order of a few thousand. A basic explanation of the operation of this filter is given with an emphasis on the similarities and differences between it and a Fourier spectrometer. Several equations that have been found to be particularly useful in designing, operating, and calibrating this filter are presented. The construction and operation of a tunable filter prototype are reported.

Introduction

The selective modulation interferometric spectrometer (SIMS)[1-10] can be optimized for operation as a tunable spectral filter. The resulting filter has a large throughput and a spectral resolving power on the order of a few thousand, which are characteristic of the SIMS. These characteristics make the filter ideally suited for measurement applications that require more spectral resolution than is obtainable with a circular variable filter but do not require the extremely high resolution characteristics obtainable with a Fabry-Perot tunable filter. For measurements requiring background suppression, the SIMS tunable filter has a potential advantage over many other types of filters since it can be configured to optically difference two input beams and provide one output proportional to this difference.[10]

This paper first discusses the theory of the SIMS configured as a tunable filter and then it discusses the construction and field testing of a prototype.

Filter Theory

The operation of the filter can be divided into two stages: 1) formation of an interferogram and 2) analysis of this interferogram. The interferogram, the Fourier transform of the source spectrum, is formed as a one-dimensional irradiance distribution: that is, each component in the spectrum contributes to the irradiance distribution a spatial component whose frequency and amplitude are proportional, respectively, to the frequency and intensity of that particular spectral component. The analysis stage consists of measuring the amplitude of the spatial component corresponding to the desired spectral component.

Interferogram formation

The lateral shearing interferometer shown schematically in Figure 1 is used to form the interferogram. The lateral shearing optical system in this interferometer shears each incident ray in two. This shearing is such that the two emerging rays are parallel and the points U' and U" on these two rays, corresponding to an arbitrary point U on the incident ray, are on a line perpendicular to the normal of the lateral shearing optical system. The lateral shear

$$s = \overline{U'\,U''} \tag{1}$$

is the same for all incident rays. The angle of the two emerging parallel rays equals the angle of the incident ray. The lateral shearing optical system introduces a path difference that depends on the angle of the incidence ray. As can be seen from Figure 1, this optical path difference is given by

$$\Delta = \overline{U''\,V} = \overline{U'\,U''} \sin\theta, \tag{2}$$

where θ is the angle of the incident ray. Thus, if second order and higher terms in θ are neglected, the optical path difference introduced by the lateral shearing optics is given

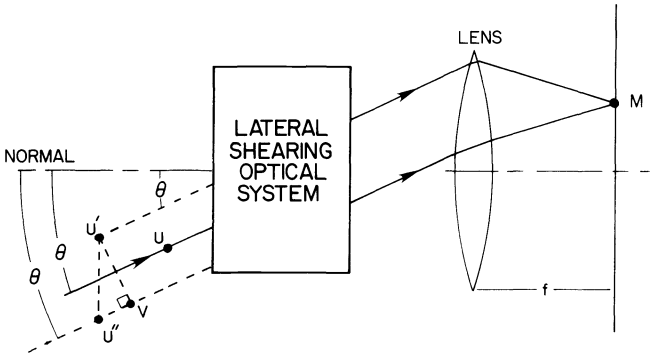

Figure 1. Schematic drawing of lateral shearing interferometer used in filter.

by

$$\Delta = s\theta. \tag{3}$$

Since for an ideal lens the optical path lengths [U'M] and [VM], shown in Figure 1, are equal, the optical path difference between the two ray paths from point U on the incident ray to point M in the focal plane of the lens is given by Equation (3). All pairs of rays that intersect at the point M have the same optical path difference. Thus, each point in the focal plane corresponds to a particular path difference. The path difference is constant along lines in the focal plane that are perpendicular to Figure 1. Thus, if an x-y coordinate system is established in the focal plane of the lens with the x axis in the plane of Figure 1, the path difference at a particular point in the focal plane can be determined from the x coordinate alone. If the optical axis of the lens is perpendicular to the lateral shearing optical system, then the optical path difference is given by

$$\Delta = \frac{sx}{f}, \tag{4}$$

where f is the focal length.

The fringes produced by the lateral shearing interferometer in Figure 1 are very similar to the fringes produced in Young's classical experiment. This similarity results because both arrangements form the far-field interference pattern for two laterally-displaced coherent sources. Thus, with a monochromatic source, the interference fringes formed across the focal plane in Figure 1 are straight, parallel, equally spaced and perpendicular to the plane of the figure. However, unlike Young's arrangement, the lateral shearing interferometer can be fabricated so that it has a very large optical throughput.

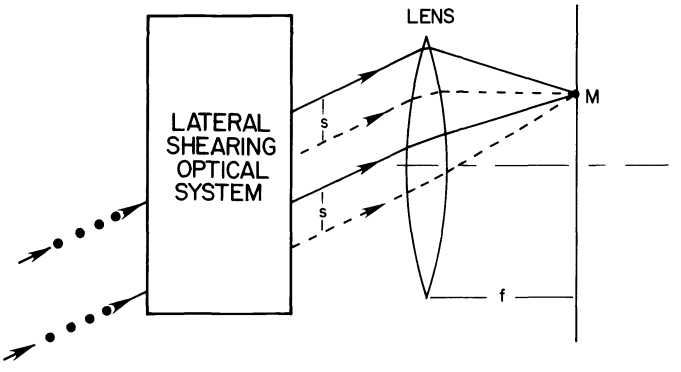

Figure 2. Illustrating the two beams of the lateral shearing interferometer.

The lateral shearing interferometer used in the filter is a two-beam interferometer. The two beams that interfere at an arbitrary point M in the focal plane of the lateral shearing interferometer are illustrated in Figure 2. The boundary of one beam is identified by solid rays; the boundary of the other beam is identified with dashed rays. If the source is monochromatic with wavelength λ, then at a point in the focal plane corresponding to an optical path difference Δ, the instantaneous complex amplitude of the electric field is given by

$$E = A_1 \exp(i\omega t + \frac{2\pi\Delta}{\lambda}) + A_2 \exp(i\omega t), \tag{5}$$

where A_1 and A_2 are the electric field amplitudes of the two beams, ω is the angular frequency and t is the time. The irradiance

$$H = CEE^*, \tag{6}$$

where C is a proportionality constant and E* is the complex conjugate of E. Thus, if the amplitudes of the two beams are equal,

$$A_1 = A_2 = A, \tag{7}$$

and if wavenumber, defined by

$$\sigma = \frac{1}{\lambda}, \tag{8}$$

is used instead of wavelength, the irradiance

$$H = 2CA^2 [1 + \cos 2\pi\sigma\Delta]. \quad (9)$$

For a polychromatic source, the irradiance is the integral over wavenumber of Equation (9) with A becoming a function of wavenumber. If the power spectral density, defined by

$$S(\sigma) = KA^2(\sigma), \quad (10)$$

where K is a constant of proportionality, is substituted in this integral, the irradiance for a polychromatic source is given by

$$H = \frac{2C}{K} \left[\int_0^\infty S(\sigma)\, d\sigma + \int_0^\infty S(\sigma) \cos 2\pi\sigma\Delta\, d\sigma\right]. \quad (11)$$

As can be seen, this equation consists of a constant term and a term that varies with the optical path difference. The varying term

$$H(\Delta) = \frac{2C}{K} \int_0^\infty S(\sigma) \cos 2\pi\sigma\Delta\, d\sigma \quad (12)$$

is called the interferogram. As can be seen, the interferogram is the cosine Fourier transform of the source spectrum. As shown in Equation (4), the optical path difference at each point in the focal plane is linearly related to its x coordinate. Therefore, Equation (12) implies that the one-dimensional variation in the irradiance at the focal plane is the Fourier transform of the source spectrum.

Equations (11) and (12) have the same form as the basic equations describing the Michelson interferometer commonly used for Fourier spectroscopy. This similarity results because both this lateral shearing interferometer and the Michelson interferometer are two-beam interferometers. However, this lateral shearing interferometer forms the entire interferogram simultaneously instead of forming the interferogram one point at a time as the Michelson interferometer does as it is conventionally used in Fourier spectroscopy.

Theoretically, the simultaneous formation of the entire interferogram by this lateral shearing interferometer could be exploited to make a multiplex spectrometer with no moving parts. The practical difficulty in making such an instrument is in taking the inverse Fourier transform of this interferogram. In theory, this could be done by measuring the irradiance distribution with a one-dimensional array of detectors and transforming the resulting measurements with a digital computer. Such an instrument would measure all spectral components simultaneously. The instrument described in this paper is much more modest; it only measures one spectral element at a time using an electro-mechanical method that will now be discussed.

Interferogram analysis

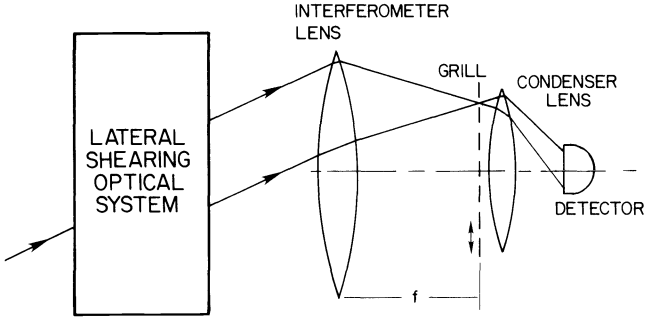

Figure 3. Optical schematic of the tunable filter.

As has been explained, the interferogram is the superposition of spatial components proportional in frequency and amplitude to corresponding spectral components that make up the spectrum. Thus, the intensity of a particular spectral component can be ascertained by measuring the amplitude of the corresponding spatial component in the interferogram. As illustrated in Figure 3, a vibrating periodic grill is located in the plane of the interferogram and the radiation passing through this grill is collected onto a detector. The spatial component of the interferogram whose spatial frequency matches the spatial frequency of the grill is modulated. Thus, the amplitude of the detector-voltage modulation is proportional to the amplitude of this spatial component and, hence, also to the intensity of the corresponding spectral component.

An expression for the correspondence between spectral and spatial components can be deduced from Equation (4) by replacing Δ with λ, the wavelength of the spectral element, and by replacing x with p, the period of the corresponding spatial component. The resulting expression

$$\lambda = \frac{sp}{f} \tag{13}$$

indicates that the spectral component that corresponds to a particular spatial frequency is determined by the shear and the focal length of the lateral shearing interferometer. Thus, by adjusting either this shear or this focal length, the spectral component to be measured is made to produce a spatial component whose spatial frequency matches that of the grill. Thus, this filter can be tuned to selectively modulate the spectral component one wishes to measure.

The grill is vibrated back and forth between a position where the grill is aligned with its matching spatial component in the interferogram and a position where the grill and this spatial component are anti-aligned or complementary. The distance between these two positions equals half the grill period. A voltage proportional to the grill displacement is used as the reference signal to synchronously demodulate the detector voltage. The output of the synchronous demodulator, which is a real-time signal, is proportional to the intensity of the tuned spectral component.

Resolution

As pointed out above, Equation (11) is the basic equation for Fourier spectroscopy. Therefore, like a Fourier spectrometer,[11] the resolution of this tunable filter, expressed in wavenumbers, is given by

$$\delta\sigma = \frac{1}{2D} , \tag{14}$$

where D is the maximum optical path difference. However, for this tunable filter the maximum path difference depends on the wavelength to which it is tuned. Since the maximum optical path difference occurs at the edge of the grill, it follows from Equation (4) that

$$D = \frac{sw}{2f} , \tag{15}$$

where w is the width of the grill. As can be seen from Equation (13), the filter is tuned by changing the ratio s/f. Thus, the maximum optical path difference depends on the wavelength to which the filter is tuned. It follows from Equations (14) and (15) that

$$\delta\sigma = \frac{f}{sw} . \tag{16}$$

Thus, the resolution of this filter is not constant with wavenumber as it is with the Michelson interferometer when used for Fourier spectroscopy. The relationship between resolution and wavenumber for this filter can be shown explicitly by using Equations (8), (13), and (16) to get

$$\delta\sigma = \frac{\sigma p}{w} . \tag{17}$$

However, it follows from Equation (17) that the resolving power defined by

$$R = \frac{\sigma}{\delta\sigma} = \frac{w}{p} = N \tag{18}$$

is a constant equal to the number of cycles N on the grill.

Equations (14) through (18) assume a rectangular grill and no vignetting. If these assumptions are not satisfied the interferogram is multiplied by a weighting function, and the effect on resolution can be ascertained using the same methods used to analyze apodization in Fourier spectroscopy.[11]

Signal-to-noise

The signal is proportional to the variation in the incident power at the detector due to the tuned spectral component. If the grill transmittance is

$$t = \frac{1}{2}[1 + \cos\frac{2\pi x}{p}] \tag{19}$$

and if its motion is a triangular function of time whose amplitude equals p/2, then this power variation is cosinusoidal as shown in Figure 4. In practice it is easier to move

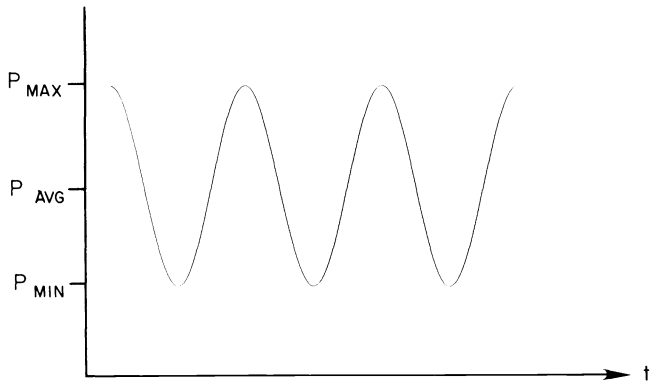

Figure 4. Time variation of the power contribution of the tuned spectral component.

the grill in a cosinusoidal fashion. When this is done, odd harmonics are generated.[9] However, the amplitude of the largest harmonic, the third, is one seventh as large as the fundamental. Therefore, even with this type of grill motion, the r.m.s. power is essentially equal to the r.m.s. power of a cosine. Thus, the r.m.s. signal current produced by an ideal photon detector is

$$i_{sig} = \frac{\lambda \eta e}{hc} \frac{(P_{max} - P_{min})}{2\sqrt{2}}, \tag{20}$$

where

η = quantum efficiency
$e = 1.6 \times 10^{-19}$ coulombs (charge on an electron)
$h = 6.62 \times 10^{-14}$ Joule sec (Planck's constapt)
$c = 3 \times 10^{8}$ meter sec^{-1} (speed of light).

From the definition of modulation efficiency, given by

$$m = \frac{P_{max} - P_{min}}{P_{max} + P_{min}}, \tag{21}$$

it follows that

$$P_{max} - P_{min} = 2m\, P_{avg}, \tag{22}$$

where P_{avg} is the average of P_{max} and P_{min}. The quantity P_{avg} is also equal to the power due to the tuned spectral element that reaches the detector when the grill is grossly misaligned. Therefore, if the grill is round,

$$P_{avg} = \left(\frac{\pi r \rho}{f}\right)^2 \tau_o \tau_g \tau_b L_{sig}, \tag{23}$$

where

r = radius of grill
ρ = radius of lateral shearing interferometer lens
f = focal length of lateral shearing interferometer lens
L_{sig} = radiance of the tuned spectral component
τ_o = transmission with the grill removed
τ_g = average transmission of grill (For the grill transmittance of Equation (19), $\tau_g = 1/2$)
τ_b = transmission factor to account for blocked rays (For an ideal filter $\tau_b = [1 - s/2\rho]^2$).

Thus, it follows from Equations (20), (22), and (23) that the r.m.s. signal current

$$i_{sig} = \frac{\lambda \eta e m}{\sqrt{2} hc} \left(\frac{\pi r \rho}{f}\right)^2 \tau_o \tau_g \tau_b L_{sig}\,. \tag{24}$$

The r.m.s. noise current caused by the random arrival of photons is given by

$$i_n = \sqrt{2eBI}, \tag{25}$$

where B is the effective noise bandwidth of the electronics and I is the average current caused by these photons. When photon noise is the dominant noise source, it is desirable to reduce the size of I by using some conventional form of filtering to reduce the spectral bandwidth of the radiation reaching the detector. If the tuned filter must operate across a broad spectral region, a filter wheel containing a selection of band-limiting filters or a circular variable filter can be used for this purpose. Let ε be defined by

$$\varepsilon = \frac{L_t}{L_{sig}}, \tag{26}$$

where L_t is the total radiance from the source radiation that lies within the spectral bandwidth of this photon-noise-limiting filter. Then, if the change in the power per photon across this spectral bandwidth is negligible, the average current due to source radiation is given by

$$I = e\left(\frac{\lambda\eta}{hc}\right)\left(\frac{\pi r\rho}{f}\right)^2 \tau_o\tau_g\tau_b\varepsilon L_{sig} \ . \tag{27}$$

It follows from Equations (25) and (27) that the r.m.s. noise current due to source radiation is given by

$$i_n = \frac{e\pi r\rho}{f}\sqrt{2\left(\frac{\lambda\eta}{hc}\right)B\tau_o\tau_g\tau_b\varepsilon L_{sig}} \ . \tag{28}$$

Other noise sources, such as photon noise from background radiation and detector noise, can be handled in the conventional fashion; that is, the total r.m.s. noise is the square root of the sum of the squares of the r.m.s. noise currents.

If photon noise from the source is the dominant noise source, the signal-to-noise ratio is the ratio of Equation (24) to Equation (28). Thus, the source-limited signal-to-noise ratio is given by

$$(SNR)_{S.L.} = \frac{m\pi r\rho}{2f}\sqrt{\left(\frac{\lambda\eta}{hc}\right)\left(\frac{\tau_o\tau_g\tau_b L_{sig}}{\varepsilon B}\right)} \ . \tag{29}$$

This equation is very useful in practice because it expresses the signal-to-noise ratio in terms of universal constants and quantities that are conveniently measured or estimated. The modulation efficiency, m, can be measured by using the tuned filter with a monochromatic extended source and by making use of either Equation (21) or (22). The modulation of an ideal filter is one half.[9] The quantities r, ρ, and f are easily measured. The product $\tau_o\tau_g\tau_b$ can be measured by twisting the grill out of alignment and calibrating the tunable filter as if it were a radiometer, its passband determined by the photon-noise-limiting filter, and then using Equation (23) with L_{sig} replaced by L_t. The quantity ε can be estimated by integrating the product of the photon-noise-limited filter response and the expected spectrum.

Lateral shearing optical system

Since tuning can theoretically be accomplished by varying either the shear or the focal length of the lateral shearing interferometer, both fixed shear and variable shear, lateral shearing optical systems are in theory usable. However, to the authors' knowledge, only the variable-shear tuning method has been used in practice. The Savart polariscope is an example of a suitable fixed-shear optical system. Fortunato[7] has used a birefringent variable-shear optical system that consists of two identical Wollaston prisms in series. The shear produced by this optical system is changed by changing the distance between these two prisms.

Fortunato[7] and the authors[9,10] have used the variable-shear optical system schematically illustrated in Figure 5. The shear in this triangular-path optical system is changed by parallel displacement of one of its mirrors. The shear

$$s = \frac{\sqrt{2}\,d}{\cos 22\tfrac{1}{2}^o} \ , \tag{30}$$

where d is the distance the translatable mirror is displaced from the position that produces zero shear. A tuning equation for a filter using this lateral optical system can be found by substituting Equation (30) in Equation (13) and solving for d. The result is

$$d = \left(\frac{f\cos 22\tfrac{1}{2}^o}{\sqrt{2}\,p}\right)\lambda. \tag{31}$$

Since the quantity within parentheses is a constant, the required mirror displacement is linearly proportional to the tuned wavelength. It is more convenient to use wavelength than wavenumber with filters that are tuned by varying the shear because of the direct proportionality between shear and wavelength expressed in Equation (13). For a filter

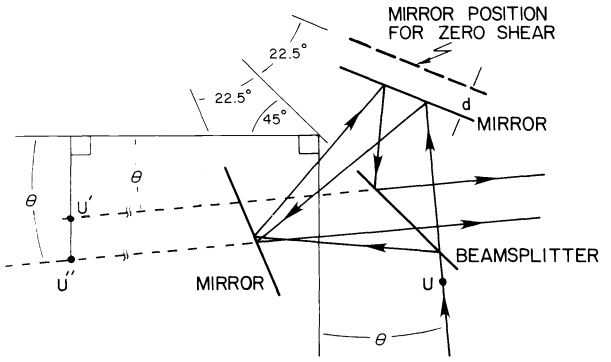

Figure 5. Schematic diagram of a cyclic, common path, lateral shearing optical system with variable shear.

tuned by varying the focal length, there would be a linear relationship between wavenumber and focal length.

The mirror displacement must be measured to an accuracy on the order of one tenth of the incremental displacement that changes the tuned wavelength by an amount equal to the resolution of the filter. It follows from differentiating Equation (31) that the incremental mirror displacement that changes the tuned wavelength one resolution element $\delta\lambda$ is given by

$$\delta d = \left(\frac{f \cos 22\tfrac{1}{2}^{\circ}}{\sqrt{2}}\right) \frac{\delta\lambda}{p} . \tag{32}$$

However, it follows from Equation (18) and the equality

$$\frac{\lambda}{\delta\lambda} = \frac{\sigma}{\delta\sigma} \tag{33}$$

that

$$\frac{\delta\lambda}{p} = \frac{\lambda}{w} . \tag{34}$$

Therefore,

$$\delta d = \lambda \left(\frac{f}{w}\right) \frac{\cos 22\tfrac{1}{2}^{\circ}}{\sqrt{2}} . \tag{35}$$

This equation is rather surprising because it implies that the incremental mirror motion required to change the tuned wavelength by one resolution element is independent of the size of this resolution element. This independence is easily seen by noting that the grill period appears in Equation (34) but not in Equation (35). However, in practice the usable grill width must often be reduced if the grill period is reduced because of aberrations in the interferometer lens. An easily remembered approximation for δd may be obtained by noting that

$$\frac{f}{w} = \frac{2}{\tan \theta_{max}} , \tag{36}$$

where θ_{max} is the maximum usable ray angle in the lateral shearing optical system, or equivalently, the angular radius of the grill. Thus,

$$\delta d = \frac{\sqrt{2} \cos 22\tfrac{1}{2}^{\circ}}{\tan \theta_{max}} \approx \frac{\lambda}{\theta_{max}} . \tag{37}$$

As can be seen from Figure 5, the same components are used by both beams. This common path characteristic is very desirable because it promotes ruggedness. The reflection and transmission coefficients of the beamsplitter should be very nearly equal, because the beamsplitter reflects one beam twice and transmits the other beam twice. Therefore, if the reflection and transmission coefficients of the beamsplitter are not equal, the two interfering beams will not be of equal strength and, consequently, the modulation efficiency will be reduced. The modulation efficiency is also reduced because the states of polarization of the two interfering beams are not identical, due to the unequal number of reflections and transmissions at the beamsplitter undergone by these two beams. A compensator equal in thickness to the beamsplitter substrate is required. Both beams pass through the beamsplitter substrate twice, but for off-axis rays the angle of the second pass is not the same for both beams. The compensator, which is located parallel to the beamsplitter, compensates for this difference. If a dielectric beamsplitter is used and two input beams are introduced on opposite sides of the beamsplitter, the tunable filter measures the difference between these two beams.[10]

Filter prototype

A tunable filter prototype was constructed and used to measure hydroxyl emissions of the night sky. A photograph of this prototype is shown in Figure 6 and some of its parameters are tabulated in Table 1.

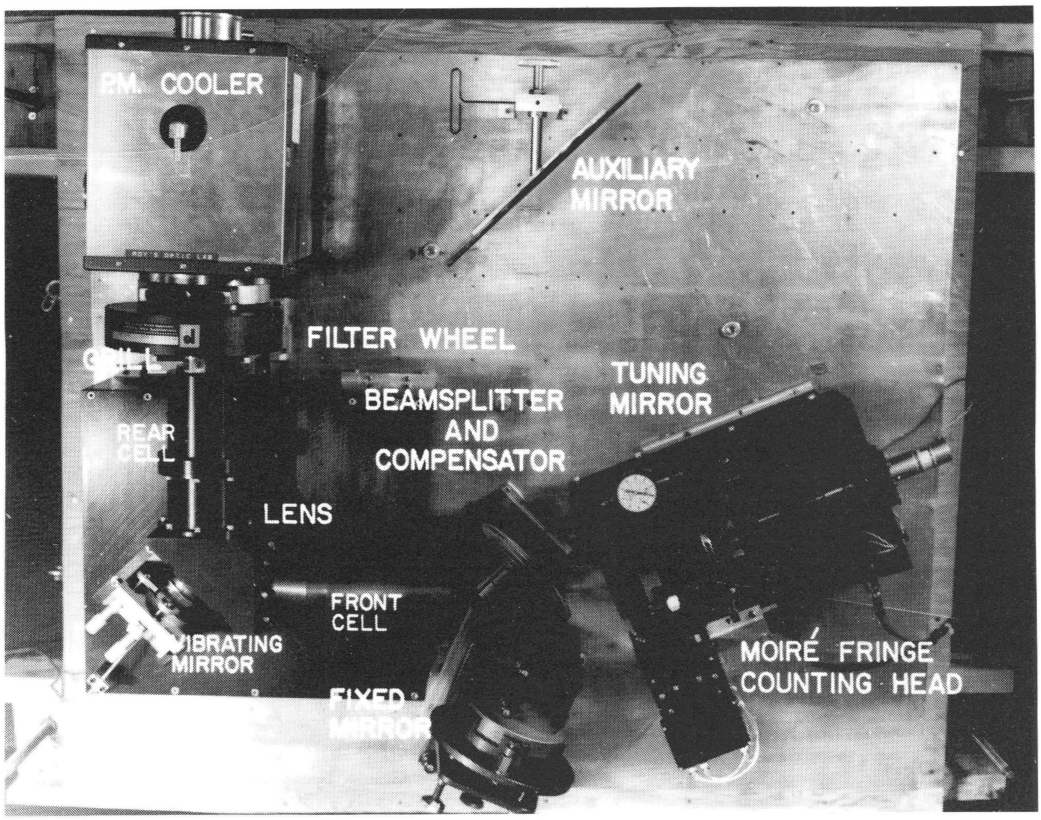

Figure 6. Tunable filter prototype with cover removed.

Table 1. Prototype Parameters

Focal length of interferometer lens	f	420 mm
Distance from exit pupil of interferometer lens to grill [For thick lens use this distance in place of f in Equations (23), (24), (27), (28), and (29)]		357 mm
Radius of exit pupil	ρ	34 mm
Radius of grill	r	14 mm
Average transmission of grill	τ_g	0.12
Modulation efficiency	m	0.2
Period of grill	p	1/50 mm

The auxiliary mirror was used to reflect night-sky emissions from the desired angular elevation into the filter. This prototype uses the variable shear optical design discussed in the previous section. The tuning mirror displacement is measured with a moiré fringe counting system that produces a fringe every 2 μm of mirror translation. The interferometer lens consists of five elements, three in the front cell and two in the rear cell. A plane mirror, which is vibrated by a piezo-electric transducer, is located between these two cells. This mirror vibration moves the interferogram back and forth across a stationary grill. Radiation is collected onto an ITT FW118 photomultiplier by a two-element condenser lens. The filter wheel, which can hold up to four photon-noise-limiting filters, is located between these two elements. For the night-sky measurements the photomultiplier was cooled to -50°C by the liquid nitrogen cooler.

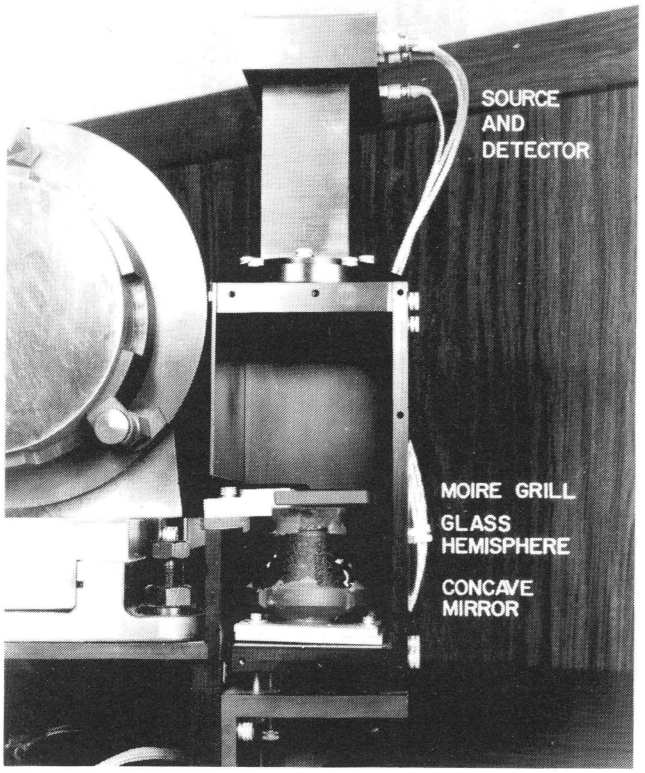

Figure 7. Moiré fringe counting head.

A close-up photograph of the moiré fringe counting head is shown in Figure 7. This type of moiré system has been described by Palmer[12], who originated it.

The spectral range is determined by aberrations in the interferometer lens. This lens was designed to have a wavefront error of less than one wave from 0.745 to 0.915 μm. Near the design center of 0.83 μm it was designed to be better than quarter wave. In order to neutralize residual distortion, the grill was made by photographing the fringes formed using a 0.6328-μm wavelength He-Ne laser as a source. The laser radiation was focused so that 1) the two primary sheared images were located in the exit pupil of the interferometer lens, 2) these two points were located equal distance from the optical axis, and 3) the line defined by these two points intersected the optical axis. These two points were located in this manner because Fortunato's[7] third-order aberration equations indicate that if this is done defocus, spherical aberration, field curvature and astigmatism will not affect the form of the fringes, which are produced by the light from these two points. This method makes it unnecessary to locate the photographic plate exactly in the focal plane, and also reduces the effects of increased aberrations that result from using radiation outside the optimized passband of the lens to expose the photographic plate. A polarizer was used when photographing the laser because this increased the fringe contrast.

Considerable vignetting was allowed because this maximized the light collecting capability that could be achieved using the available lens and beamsplitter-compensator pair. It was necessary to accept this vignetting because of a basic physical limitation of the triangular lateral shearing optical system. This limitation is that the triangle must be large in order to get the beams past the end of the beamsplitter-compensator pair, but then this pair acts as two apertures separated by a large distance. Thus, the diameter of the beamsplitter-compensator pair must be considerably larger than the entrance pupil of the interferometer lens if vignetting is to be avoided. The beamsplitter-compensator pair used in the prototype are 150 mm in diameter. This problem is even worse if the entrance pupil is located a considerable distance behind the first lens surface as it is for the interferometer lens used in the prototype. Fortunato[7] has suggested that this limitation may be circumvented if instead of going past the end of the beamsplitter-compensator pair, the two beam pass through the pair.

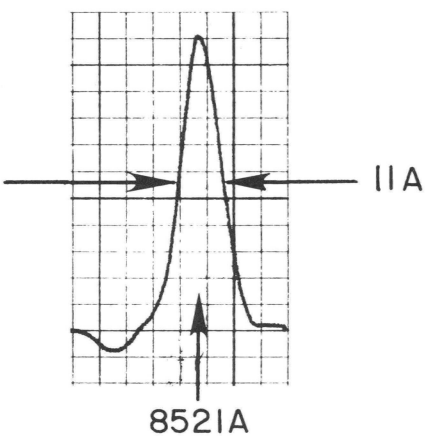

Figure 8. Measured instrument function of the filter.

The prototype filter was taken to a remote site to measure upper atmospheric airglow emissions. The instrument function measured at this site using the 8521-angstrom line of a cesium lamp is shown in Figure 8. This instrument function is 11 angstroms wide at fifty percent of its peak value. Thus, the measured resolving power was 775. Measurements made with the prototype of night sky emissions at 8430, 8415, and 8400 angstroms, which correspond approximately to the wavelengths of the $P_1(3)$, $P_2(3)$, and $P_1(2)$ lines of the OH (6-2) transition are shown in part (a) of Figure 9. A synthetic hydroxyl spectrum that was computed using a rotational temperature of 250°K and a triangular instrument function 11 angstroms wide at its fifly percent points is shown in part (b) of this figure. The photon-noise-

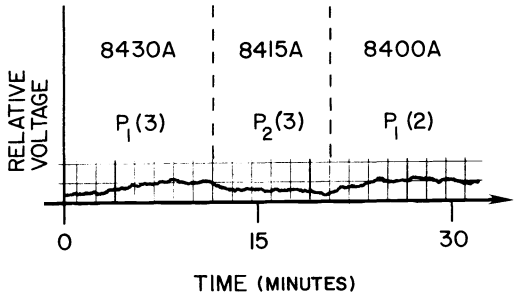

(a)

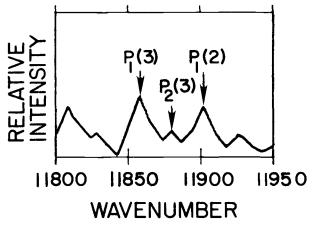

(b)

Figure 9. Prototype measurements of night-sky hydroxyl emissions compared to a synthetic spectrum.
(a) Filter output voltage, with a time constant of 5 minutes, for tuned wavelengths corresponding to the $P_1(2)$, $P_2(3)$, and $P_1(3)$ lines of the OH(6-2) transition.
(b) Synthetic spectrum assuming an OH rotational temperature of 250°K and a triangular instrumental profile with a half width equal to that of the tunable filter.

limiting filter used to make these measurements was a bandpass filter with 50 percent band edges at 8570 and 8160 angstroms. An ε value of 22 was estimated from this bandwidth, the bandwidth of the tunable filter, and the OH spectrum. The measurements were made using a five minute time constant. The tunable filter was tuned to each wavelength in turn for approximately two time constants; the tuning time was insignificant compared to the time constant. As can be seen, the filter output voltage increased while the filter was tuned to 8430 angstroms, decreased while tuned to 8415 angstroms, and increased again while tuned to 8400 angstroms. Thus, it can be concluded that the filter detected the approximate 3×10^{-12} watts/cm^2-sr radiance levels of the $P_1(2)$ and $P_1(3)$ lines and that these lines, which are 30 angstroms apart, were resolved.

The two main problems experienced in field testing this prototype were the following: 1) the grill and the interferogram would remain in proper registration for only a short period of time, and 2) the optical quality of the interferometer lens, which forms the interferogram, became inadequate if the temperature dropped below 12°C. The major cause of the first problem seems to be creep in the piezoelectric transducer that was used. This could be corrected by using feedback. The second problem is confirmation that the interferometer lens must be very well corrected if moderate resolving powers are to be achieved.

Conclusion

It has been shown that a tunable spectral filter with a large optical throughput and a resolving power on the order of a thousand can be made by using the selective modulation interferometric spectrometer (SIMS) technque. Further work is needed to ascertain how well the practical problems experienced with the prototype can be circumvented. The major problem areas are associated with the interferometer lens and the grill. Since the two interfering beams are combined after passing through the interferometer lens, the aberrations of this lens must be very small. The low modulation efficiency of the grill is a limitation because the signal-to-noise ratio is proportional to the modulation efficiency. For operation of the filter at wavelengths longer than approximately one micrometer, computational techniques can be used to make the grill. It is possible to eliminate the grill, for example, by using a detector array, thereby eliminating the problems associated with the grill.

Acknowledgments

The authors wish to thank Donald P. Saletnik for his excellent, dedicated assistance in the design, fabrication, and testing of the prototype. Thanks also go to Charles W. Eastman for programming the computer routine to generate the synthetic spectrum, to Charles P. Dolan, Jr. for preparing the art work, and to Helene A. Alterio for doing the typing.

Funding for this work was provided by the Air Force Office of Scientific Research (AFOSR)

References

1. Prat, R., "Nouvelle méthode spectrométrique interférentielle," *Jap. J. Appl. Phys.*, vol. 4, supplement *I*, pp. 448-450. 1965.

2. Prat, R., "Spectrométrie et spectrographic interférentielles par dédoublement achromatique transversal de la source. *I*," *Opt. Acta.*, vol. 18, pp. 213-244. 1971.

3. Prat, R., "Spectrométrie et spectrographic interférentielles par dédoublement achromatique transversal de la source. *II*," *Opt. Acta.*, vol. 18, pp. 247-268. 1971.

4. Fortunato, G. and A. Maréchal, "Spectromètre interfértiel à modulation sélective," *C. R. Acad. Sci., B*, vol. 274, pp. 931-934. 1972.

5. Maréchal, A. and G. Fortunato, "Recent Developments in Selective Modulation Spectrometry," In *Space Optics: Proceedings of the Ninth International Congress of the International Commission for Optics*, (B. J. Thompson and R. R. Shannon, editors), National Academy of Sciences, Washington D.C. 1974.

6. Fortunato, G. and A. Maréchal, "Possibilités de dérivation et de corrélation de spectres dan les spectromètres interférentiels à grille," *C. R. Acad. Sci., B*, vol. 276, pp. 527-530.

7. Fortunato, G., "Etude d'un spectromètre interférentiel à modulation sélective: applications," Thèse de doctorat ès-sceinces physiques présentèe a l'université paris sud centre d'orsay. 1976.

8. Fortunato, G. "Application de la corrélation interférentielle de spectres a la détection de polluants atmosphériques," *J. Optics (Paris)*, vol. 9, pp. 281-290. 1978.

9. Esplin, R. W., "The Selective Modulation Interferometric Spectrometer," *Opt. Eng.* vol. 17, pp. 73-81. 1978.

10. Vanasse, G. A., R. W. Esplin, and R. J. Huppi, "Selective Modulation Interferometric Spectrometer (SIMS) Technique Applied to Background Suppression," *Opt. Eng.*, vol. 18, pp. 403-408. 1979.

11. Vanasse, G. A. and H. Sakai, "Fourier Spectroscopy," In *Progress in Optics*, (E. Wolf, editor), vol. 6, North-Holland, Amsterdam. 1967.

12. Palmer, D. A., "Moiré Fringe Reading Head for Use with a Fine Grating," *J. Sci. Instr.*, vol. 37, pp. 261-262. 1960.